

Quantification of B_0 and B_1 Effects on the Estimation of MT Parameters at 3.0 T

M. Cercignani¹, M. R. Symms², P. A. Boulby², G. J. Barker³

¹NMR Research Unit, Institute of Neurology, UCL, London, England, United Kingdom, ²Dept of Clinical and Experimental Epilepsy, Institute of Neurology, UCL, London, England, United Kingdom, ³Dept of Clinical Neuroscience, CNS, Institute of Psychiatry, King's College London, London, England, United Kingdom

Introduction

Quantitative magnetization transfer (MT) imaging relies on fitting a non-linear model to a series of MT-weighted images collected with MT pulses of variable amplitude (ω) and offset frequency (Δ). Any imperfection in the B_1 field results in a deviation from the nominal value of ω , while any imperfection in the B_0 field results in a deviation from the nominal value of Δ . As a consequence, field inhomogeneities can introduce a spatially variable bias in the estimated parameters (1). These effects are expected to be more pronounced at 3.0 T than at 1.5 T. The aim of this work was to quantify the error introduced by B_1 and B_0 field inhomogeneities into the MT parameters estimated from data collected at 3.0 T.

Methods

This work is based on the model of quantitative MT developed by Ramani et al. (2). In Ramani's model, the MT pulse is replaced by continuous wave irradiation with the same mean square amplitude (continuous wave power equivalent, or CWPE, approximation). Six independent quantities can be derived from the model: RM_0^A , $f/R_A(1-f)$, T_2^B , $1/R_A T_2^A$, R_B , and gM_0^A . Here A and B label the liquid and the semisolid pools, respectively, and f represents the bound proton fraction (2), which can be extracted after the fitting by further processing (2) if an independent measure of T_1 is available.

One subject (male, 39 years) was scanned on a 3.0 T system using a 3D MT-weighted fast SPGR sequence (A) (TR/TE=25.8/2.7 ms, flip angle=5°, Gaussian MT pulses, duration=14.6 ms), which collects 10 volumes with 5 values of Δ (ranging from 0.4 to 20 kHz) for 2 values of ω (219 and 656 rad s⁻¹). In addition to the MT data, (B) two 4-shot spin-echo EPIs (TR/TE=15000/20 ms, flip angles=60° and 120°, matrix 64x64), (C) 2 fast 3D SPGRs (TR/TE1/TE2=25.8/2.7/5.4 ms, flip angle 5°) and (D) 3 fast 3D SPGRs (TR/TE=6.0/2.8 ms, flip angles 15°, 7°, and 3°) were collected to map B_0 , transmit B_1 , and T_1 , respectively. Acquisition matrix (256x96), FoV (24x18 cm²) and number of slices (28) were the same for all sequences unless otherwise specified. Slice thickness was 5 mm for all the SPGR sequences and 4 mm with 1 mm gap for the EPI. After image co-registration, B_1 maps were obtained from sequence B using the double angle method (3) and the resulting maps were smoothed using a 3rd order polynomial fitting. Maps of the B_0 deviation from the value in the centre of the head were calculated from the phase images obtained from sequence C (4). T_1 maps were calculated by fitting the signal in sequence D as a function of the flip angle, after it was corrected on a pixel-by-pixel basis for B_1 inhomogeneities (5). Finally, since B_0 and both transmit and receive B_1 inhomogeneities also cause the signal intensity (and therefore the SNR) in the MT weighted images to vary with position, the least MT-weighted volume (from sequence A) was convolved with a low-pass filter to produce a map of the slowly varying signal intensity (independent of the anatomy). A map of the local signal intensity standard deviation (SD) was obtained by taking the inverse of this image. Ramani's model was then fitted to the data 4 times using the Marquardt-Levenberg algorithm (keeping R_B fixed and equal to 1, and modelling the semisolid pool absorption lineshape with a super-Lorentzian): 1) without any correction; 2) correcting ω only for B_1 inhomogeneities; 3) correcting both ω (for B_1) and Δ (for B_0); and 4) finally, correcting both ω and Δ and accounting for the pixel-by-pixel varying SD in the fitting algorithm. f maps were extracted from the fitted data as previously described (2).

Results

Typical B_1 , B_0 and SD maps are shown in Fig 1. The parameters estimated by the fourth fitting (performing all three corrections) were used as gold standards to estimate the pixel-by-pixel percentage error in the MT parameters (RM_0^A , T_2^B , $1/R_A T_2^A$, and f) estimated by the other three procedures. Excluding the information from the local SD did not result in changes of more than 1% in any of the parameters. f estimates appeared particularly robust to B_0 field inhomogeneities, only showing minimal errors in areas where the change in magnetic susceptibility is abrupt. Conversely, B_1 field variations resulted in errors as large as 50% or more. An opposite pattern characterised T_2^B estimates, which appeared more sensitive to B_0 than to B_1 field inhomogeneities. For T_2^B , the error was in any case within 10% in most areas of the brain. Both B_0 and B_1 field inhomogeneities significantly affected the estimates of RM_0^A and $1/R_A T_2^A$. (see Fig 2). Examples of f maps obtained with and without correction are shown in Fig 3. The use of field-map correction considerably improves the uniformity of signal intensity across the image.

Discussion

We have shown that accounting for both static and RF magnetic field inhomogeneities is essential to obtain reliable estimates of MT parameters at 3.0 T. If interested in the estimation of f only, however, B_0 field mapping can be skipped in the interest of time. While collecting maps of the relative B_1 and B_0 field variation is relatively easy, it would be more desirable to obtain an estimate of the absolute field strength. This is more challenging and not always feasible. Accounting for the relative variation is, however, an important preliminary step that allows the quantitative comparison between MT parameters measured in different areas of the brain.

References

1. Sled JG and Pike GB, Magn Reson Med 2001; 46: 923-31.
2. Ramani A, et al. Magn Reson Imaging 2002; 20: 721-31.
3. Stollberger R and Wach P, Magn Reson Med 1996; 35: 246-51.
4. Cusack and Papadakis, NeuroImage 2002; 16: 754-64.
5. Venkatesan R et al. Mag Reson Med 1998; 40:592-602

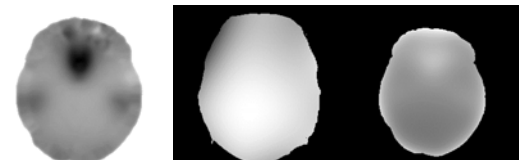


Fig 1. B_0 (left), B_1 (centre) and SD (right) maps of the same slices (Note that B_0 and B_1 maps extend to the skull, while SD maps is masked to include the brain only).

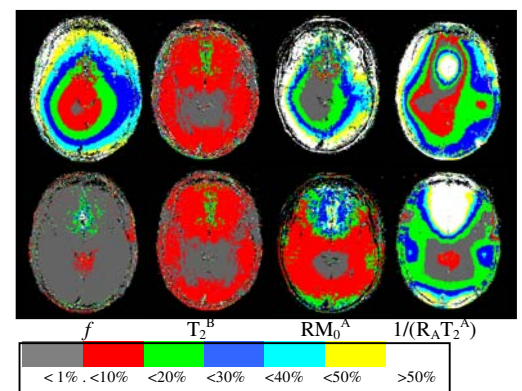


Fig 2. Maps of the percentage error in the estimated MT parameters when neither B_1 nor B_0 correction is performed (top) and when only B_1 but no B_0 correction is performed (bottom).

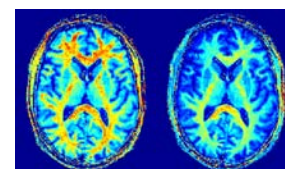


Fig 3. f maps calculated with both B_1 and B_0 correction (left) and with no correction (right).